Scientific paper

Influence of the Synthesis Parameters on the Properties of $NaYF_4$:Yb^{3+},Tm^{3+} Nanoparticles

Olivija Plohl,[1,2,*] Boris Majaron,[3] Maja Ponikvar-Svet,[4] Darko Makovec[1] and Darja Lisjak[1]

[1] *Department for Materials Synthesis, Jožef Stefan Institute, Jamova cesta 39, 1000 Ljubljana, Slovenia*

[2] *Jožef Stefan International Postgraduate School, Jamova cesta 39, 1000 Ljubljana, Slovenia*

[3] *Department of Complex Matter, Jožef Stefan Institute, Jamova cesta 39, 1000 Ljubljana, Slovenia*

[4] *Department of Inorganic Chemistry and Technology, Jožef Stefan Institute, Jamova cesta 39, 1000 Ljubljana, Slovenia*

* *Corresponding author: E-mail: olivija.plohl@ijs.si*

Received: 09-03-2015

Abstract

Fluorescent nanoparticles, especially fluorides, have received a great deal of interest due to their optical properties, making them suitable for applications in bio-imaging. For this reason they need to exhibit a superior chemical stability in aqueous media. We have studied the influence of the synthesis parameters on the chemical stability of $NaYF_4$ nanoparticles co-doped with Yb^{3+} and Tm^{3+}. These nanoparticles have different crystal structures, and were synthesized hydrothermally or with thermal decomposition. The samples were characterized with X-ray diffraction and transmission electron microscopy. The up-conversion fluorescence of nanoparticles dispersed in water was measured at 400–900 nm. The partial dissolution of the fluorine in water was detected with an ion-selective electrode for all the samples. The dissolution of the other constituent ions was analysed with an optical emission spectrometer using inductively coupled plasma. The nanoparticles with a hexagonal crystal structure and sizes of around 20 nm that were synthesized with thermal decomposition showed a superior chemical stability in water together with a superior up-conversion fluorescence yield.

Keywords: Nanoparticles, dissolution, fluorescence, up-conversion

1. Introduction

Recent progress in science has resulted in the greater availability of enhanced, sensitive techniques, in particular, advanced techniques for fluorescence imaging.[1] Despite the remarkable applicability of traditional fluorescent dyes, their current use is limited by the presence of auto-fluorescence, narrow absorption and broad emission spectra, short detection times due to photobleaching, and chemical degradation.[2,3] Therefore, to meet the demands of modern diagnostics, the development of advanced fluorescence probes is essential. Recently, the conversion of near-infrared (NIR) excitation into visible or NIR light via nonlinear optical processes, refereed to as up-conversion (UC), has generated a lot of interest among researchers. Rare-earth (RE) doped UC nanoparticles (UCNPs) serve as an alternative and excellent substitute for traditional fluorescent dyes.[4] These RE-doped UCNPs can be excited by NIR light and possess several advantages, which include excitation via a low-power NIR laser or diodes, deeper NIR light penetration into the biological tissue, causing less photo damage to biological samples, and improved detection sensitivity owing to the absence of auto-fluorescence.[4–9] RE-doped UCNPs have demonstrated great potential in many fields of biomedical science for bio-detection, bio-imaging, multiplexed analysis or therapy.[10–13]

Fluorides such as $NaYF_4$ have attracted considerable attention as a suitable host matrix. The crystal structure of $NaYF_4$ exhibits two polymorphic forms, i.e., the cubic (α-) and hexagonal the (β-). The hexagonal structure of $NaYF_4$ has three cation sites, one for the RE ions (1a), another for the RE and Na ions (1f), and a third for the Na ions (2h). The sites 1a and 1f both have C_{3h} symmetry, whereas the 2h site has C_s symmetry.[14] Among the fluoride materials, β-$NaYF_4$ is considered to be one of the most

efficient materials for the UC process when sensitized with Yb^{3+} and activated by Er^{3+} or Tm^{3+} ions.[15,16] Much effort has been focused on the synthesis of $NaYF_4$ NPs with different sizes and morphologies. For instance, hexagonal microprisms with a remarkably uniform morphology and submicron size of β-$NaYF_4$:Yb^{3+},Er^{3+} UCNPs were synthesized hydrothermally.[14,16] Although hydrothermal synthesis is an environmentally friendly and solution-based, single-step synthesis, it typically yields UCNPs with submicron sizes that are inappropriate for bio-applications. Capobianco *et al.*[17] developed a method based on the thermal decomposition of metal organic complexes in hydrophobic, high-boiling-point solvents for the synthesis of monodispersed β-$NaYF_4$:Yb^{3+},Er^{3+}/Tm^{3+} NPs with a controllable size, shape and phase, which are appropriate for bio-applications. Prasad *et al*. introduced $NaYF_4$:Yb^{3+},Tm^{3+} NPs as *in vitro* and *in vivo* NIR-to-NIR UC probes.[18]

However, as a newly emerging nanomaterial, the potential health risks of the $NaYF_4$:Yb^{3+},Er^{3+}/Tm^{3+} UCNPs have not been adequately investigated.[19] The studies on the potential leakage of the RE^{3+} or the F^- from the fluoride UCNPs in the water and the potential (cyto)toxicity in a biological environment were limited and tended not to reveal any significant cytotoxicity.[20–23] Nevertheless, greater concern should be paid to the long-term toxicity effects of RE^{3+} and F^-, which might be released from fluoride UCNPs. For example, Gd ions released from Gd-based MRI contrast agents were reported to induce nephrogenic systemic fibrosis.[24] Wang *et al.*[22] encapsulated UCNPs within a CaF_2 shell to supress the leakage of RE^{3+} from UCNPs in a buffer solution to ensure their biocompatibility. Several investigations demonstrated that fluoride ions can induce oxidative stress and modulate intracellular redox homeostasis, cause apoptosis and alter gene expression.[25]

Due to the limited toxicological data available for fluoride UCNPs, the aim of this work was to synthesize $NaYF_4$:20%Yb^{3+},2%Tm^{3+} UCNPs and to analyse their chemical stability in aqueous media and to correlate this with the UC emission properties.

2. Experimental

2. 1. Materials

All the reagents were used as received, without any additional purification. $RECl_3 \times XH_2O$ [RE = Y(99.99%), Yb (99.9%), Tm (99.9%)], $Ln(NO_3)_3 \times XH_2O$ [RE=Y (99.9%), Yb (99.9%), Tm (99.9%)], NaF (99%), NH_4F (98%), oleic acid (OA, 90%), 1-octadecene (ODE, 90%), and citric acid (CA, 99%) were all purchased from Alfa Aesar. NaOH (≥99%) and methanol were purchased from Merck. Ethanol (≥99.9%), acetone (99.8%) and hexane (>95%) were purchased from CarloErba Reagents. HCl and diethyl ether (DE, 99.5%) were purchased from Aplichem. The water used for the synthesis was deionized. To ensure the proper stoichiometry of the product, the Ln^{3+} content in the reagent nitrates and chlorides was determined using an optical emission spectrometer with inductively coupled plasma (ICP-OES, Agilent 720).

2. 2. Synthesis

The hydrothermal synthesis (HT) of the $NaYF_4$:20%Yb^{3+},2%Tm^{3+} UCNPs was carried out as described in detail elsewhere[14]. In short, 2 mmol of RE nitrates in a stoichiometric ratio were dissolved in 9 ml of deionized water. This solution was admixed to an 18 ml aqueous solution containing 8 mmol Na_3(cit) (the molar ratio of citrate ion:Ln^{3+} was 4:1). The Na_3(cit) was prepared by dissolving a stoichiometric ratio of NaOH and CA in deionized water. After vigorous stirring for 30 min, 27 ml of aqueous solution containing 25 mmol of NaF, was admixed to the above solution and transferred into a 70- ml-Teflon vessel in a stainless-steel autoclave, and heated at 3 °C/min to 180 °C with a soaking time of 1–20 hours (Table 1). As the autoclave was cooled to room temperature naturally, the precipitates were separated by centrifugation at 5000 rpm for 5 min, washed with ethanol and deionized water and then dried in air or kept in a water suspension.

The thermal decomposition (TD) synthesis of the $NaYF_4$:20%Yb^{3+},2%Tm^{3+} UCNPs was carried out as before, but using some modifications.[26] Here, 2 mmol of stoichiometric amounts of RE chlorides were weighed into a 100 ml flask. After that, 12 ml of OA and 30 ml of ODE were added to the solution, which was heated to 156 °C for 30 min under an Ar atmosphere and then cooled to room temperature. Next, a solution of 8 mmol of NH_4F and 5 mmol of NaOH in 10 ml of methanol was added and maintained at 50 °C for 30 min. After the evaporation of the methanol, the solution was heated to 300 °C under an Ar atmosphere for 1.5 h and then cooled to room temperature (Table 1). The UCNPs were precipitated with acetone, collected after centrifugation (at 5000 rpm for 5 min), washed with ethanol, to remove the excess of oleic acid, and with deionized water, to remove the NaCl and re-dispersed in hexane.

Oleate-capped $NaYF_4$:20%Yb^{3+},2%Tm^{3+} UCNPs from the TD synthesis in hexane were transferred into an aqueous phase using a modified ligand-free protocol.[27]

Table 1: UCNPs synthesis parameters.

Synthesis	T/°C	t/h	n(Cit^{3-}):n(Ln^{3+})	PEG 1500/g
A-HT	180	20	4:1	/
B-HT	180	10	4:1	/
C-HT	180	1	4:1	/
D-HT	180	10	4:1	0.5
TD	300	1.5	/	/

Typically, $NaYF_4$:20%Yb^{3+},2%Tm^{3+} UCNPs, dispersed in 10 ml of hexane, were first dried. Water (10 ml) was then added to the dried UCNPs and the pH value was decreased to 2–4 using 0.1 M HCl. The mixture of UCNPs and water was sonicated in an ultrasonic bath for about 4 h, while maintaining a pH value of 2–4 by adding 0.1 M HCl every 30 min. The carboxylate groups of the oleate ligand were gradually protonated to yield free OA. After the completion of this process, the aqueous solution was mixed with DE to remove the OA by extraction. The procedure was repeated several times until the solution became totally transparent. The ligand-free $NaYF_4$:20%Yb^{3+},2%Tm^{3+} UCNPs in water were recovered by a centrifugation at 5000 rpm for 5 min. The product was then immersed in acetone, centrifuged at 5000 rpm for 5 min, and then finally dispersed in deionized water.

2. 3. Characterization

The crystal structure of the as-synthesized UCNPs was verified by X-ray diffraction (XRD) with an X-ray diffractometer (Philips X'Pert PRO MPD Diffractometer, PANanalytical using CuKα radiation, $\lambda_{CuK\alpha 1}$ = 1.5406 Å). The crystallite sizes were determined from the X-ray diffractograms using the Pawley method[28] with the crystallographic program Topas2R 2000 (Bruker, AXS). The morphology of the UCNPs was inspected with a transmission electron microscope (TEM, Jeol 2100) and a scanning electron microscope (FEG-SEM, Jeol 7600). The TEM samples were prepared by dropping a diluted dispersion of UCNPs onto the surface of a copper grid. The equivalent diameters of the UCNPs were determined from their surfaces using Gatan Digital Micrograph Software. A minimum of 150 UCNPs per sample was counted for the statistics. Energy dispersive X-ray spectroscopy (EDXS) and selected area electron diffraction (SAED) were also performed during the TEM analyses.

The concentration of UCNPs in the suspension was determined thermogravimetrically. The water was evaporated at 70 °C over night and the organic species (citrate) were decomposed during heating (3 °C/min) to 500 °C with a holding time of 1 h. The UC emission of the UCNPs was characterized for irradiation with a continuously emitting, 978 nm-diode laser. Focusing of the laser beam with an average power of 2 W produced an irradiant power density of ~160 J/cm^2. The resulting UC fluorescence was collected at an angle of ~90° with respect to the beam axis and analyzed using a compact spectrometer (USB4000, Ocean Optics) in the spectral range 400–900 nm.

The dissolution analyses were performed from three-days old aqueous suspensions. These suspensions were prepared from the as-synthesized nanoparticles, which were washed as described above. The washing procedure reassured that all the synthesis residuals were eliminated and that pure nanoparticles were used in the dissolution experiments. The solutions for the analyses were prepared by the centrifugation of suspensions at 5000 rpm for 5 min to remove a major fraction of the UCNPs followed by ultrafiltration using a filter (MW 30kDa) to eliminate any remaining UCNPs from the solution. The so-prepared solutions were used for the analysis of the dissolved ions. An Orion 960 Autochemistry System with a temperature sensor and a combined fluoride ion selective electrode (Thermo, Orion model 96–09) were used for the potentiometric determination of the F^- using the multiple known addition method with a blank subtraction.[29] The concentration of the dissolved cations (Yb^{3+}, Tm^{3+}, Y^{3+} and Na^+) was determined with ICP-OES.

3. Results and Discussion

The structure and phase purity of the products were first examined by XRD (Figure 1). Under hydrothermal conditions, $NaYF_4$ crystallizes first in a metastable cubic (-α) structure and then transforms into a thermodynamically stable hexagonal (β-) structure after a prolonged synthesis time.[30] The phase transformation process during the HT synthesis was examined within a reaction time of 1–20 h (Table 1) at a temperature of 180 °C. The sample obtained after a 1-h reaction time (C-HT) shows a pure cubic, α-$NaYF_4$ structure (JCPDS 77–2042). When the reaction time was increased to 10 or 20 h (A-HT, B-HT) minor XRD peaks of the β-$NaYF_4$ structure were observed in addition to those of the α-$NaYF_4$ structure (see the enlargements in Figure 2). This indicates that the structure of the NPs partially transformed from the α to the β phase with a prolonged reaction time. However, this transformation was not significant since the relative intensities of the XRD peaks of the β-$NaYF_4$ were very low. Despite the 10-h synthesis time no transformation to β-$NaYF_4$ was

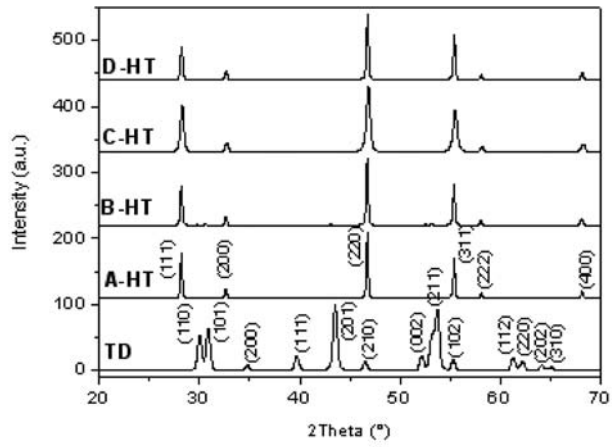

Fig. 1: XRD patterns of the as-synthesized UCNPs. The indices correspond to β-$NaYF_4$ (JCPDS 16-0334 for TD) and α-$NaYF_4$ (JCPDS 77-2042 for the A-HT, B-HT, C-HT and D-HT samples).

Table 2: Basic properties and the dissolution data of the synthesized UCNPs.

Sample name	Crystal structure	Crystallite size (nm)	NPs size (nm)	Conc. UCNPs in the suspension (mg/ml)	Conc. Dissolved ions (μg/ml)	Dissolved ions per formula unit (mol.%)
A-HT	α+β-$NaYF_4$	120 ± 10 (α-$NaYF_4$) 120 ± 50 (β-$NaYF_4$)	1135 ± 25	4.1	Na: 29.0 ± 0.1 Y: 7.22 ± 0.02 Tm: 0.67 ± 0.02 Yb: 7.90 ± 0.02 F: 16.6 ± 0.2	**Na: 6.3** **Y: 0.52** **Tm: 1.0** **Yb: 1.15** **F: 1.1**
B-HT	α+β-$NaYF_4$	94 ± 5 (α-$NaYF_4$) 95 ± 20 (β-$NaYF_4$)	160 ± 13	6	Na: 33.7 ± 0.1 Y: 3.49 ± 0.02 Tm: 1.20 ± 0.02 Yb: 5.49 ± 0.02 F: 19.0 ± 0.2	**Na: 5** **Y: 0.17** **Tm: 1.0** **Yb: 0.5** **F: 0.85**
C-HT	α-$NaYF_4$	80 ± 4	103 ± 10	2.8	Na: 17.0 ± 0.1 Y: 1.85 ± 0.02 Tm: 0.15 ± 0.02 Yb: 0.97 ± 0.1 F: 9.9 ± 0.1	**Na: 5.4** **Y: 0.19** **Tm: 0.3** **Yb: 0.2** **F: 0.94**
D-HT	α-$NaYF_4$+NaF	30 ± 1	32 ± 6	3.4	Na: 139.1 ± 0.5 Y: 12.5 ± 0.1 Tm: 3.54 ± 0.02 Yb: 33.5 ± 0.1 F: 69.1 ± 0.2	**Na: 36.7** **Y: 1.1** **Tm: 6.4** **Yb: 5.9** **F: 5.5**
TD	β-$NaYF_4$	30 ± 1	21 ± 3	1.3	Na: 3.22±0.02 Y: 0.33±0.02 Yb: 0.20±0.02 Tm: 0.04±0.01 F: 1.8±0.2	**Na: 2.2** **Y: 0.08** **Yb: 0.09** **Tm: 0.19** **F: 0.38**

detected with the XRD for the D-HT sample. This can be attributed to the PEG, which was added during the synthesis and affected the reaction kinetics. In contrast to the HT samples, the pure β-$NaYF_4$ phase was obtained with the TD synthesis. No second phase was detected in the XRD pattern (Figure 1), revealing that the Yb^{3+}/Tm^{3+} ions have been effectively incorporated into the host lattice of the $NaYF_4$.

The TEM images (Figure 3) show the differences in the morphologies between the different UCNPs. The A-HT UCNPs have an anisotropic, truncated, cube-like morphology (see Figure 4) and they are of micron size. The B-HT and C-HT UCNPs are quasi-spherical with sizes of around 100–200 nm (Table 2). The significantly smaller size (around 30 nm) of the D-HT UCNPs suggests that the PEG inhibits the crystal growth dynamics. The

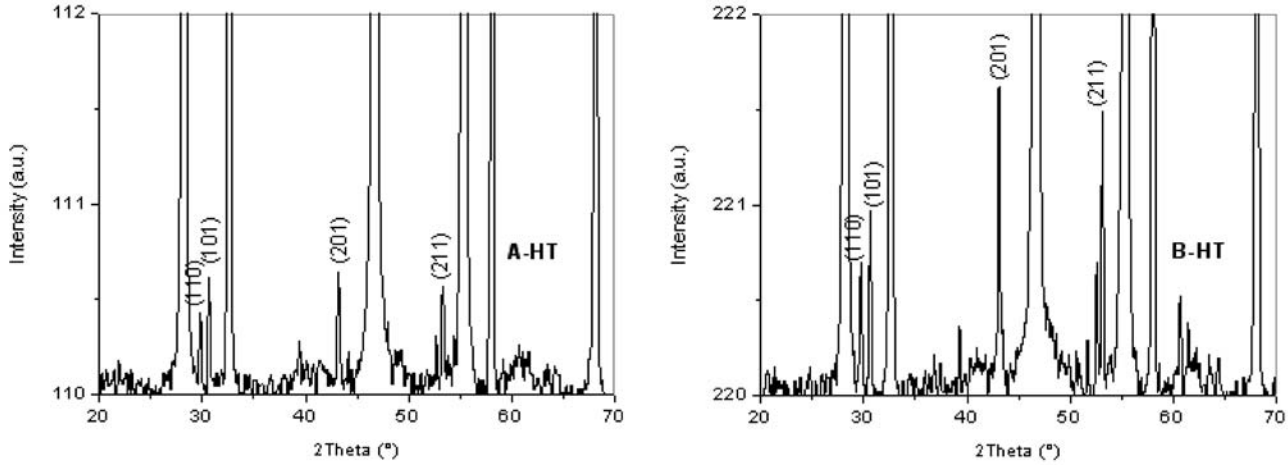

Fig. 2: Enlargements of the XRD patterns for the A-HT and B-HT samples. The indices correspond to β-$NaYF_4$ (JCPDS 16-0334).

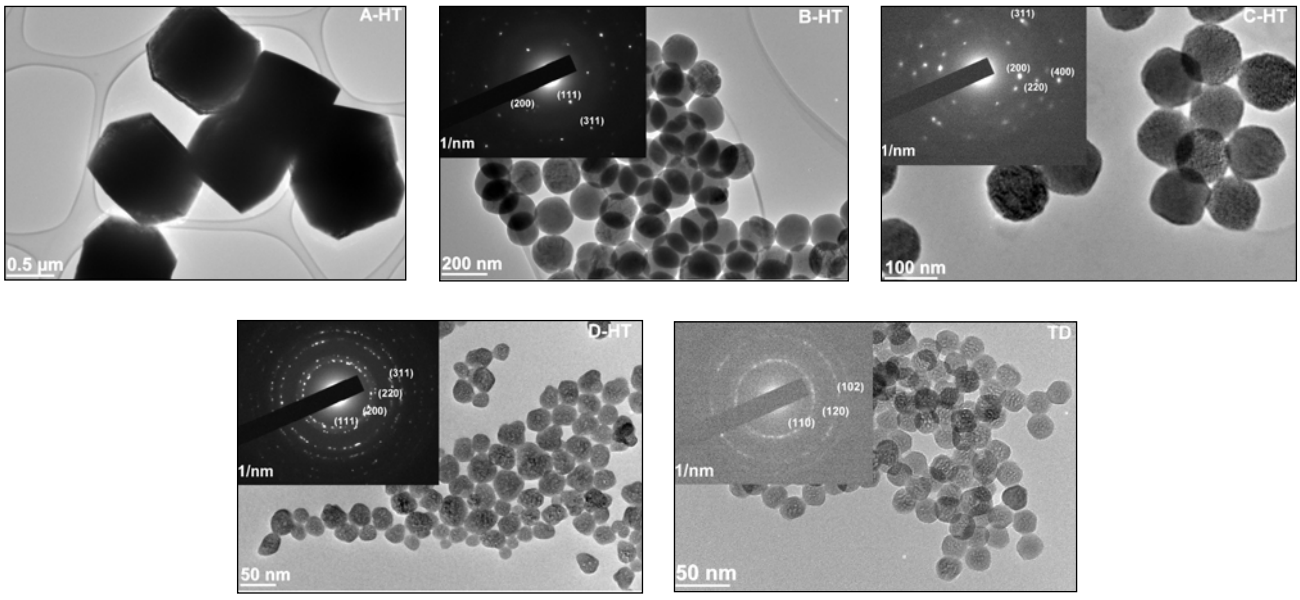

Fig. 3: TEM images of the as-synthesized UCNPs. The corresponding SAED are indexed according to α-$NaYF_4$ (A-HT, B-HT. C-HT and D-HT) and β-$NaYF_4$ (TD).

TD UCNPs are quasi spherical and with a relatively homogeneous size of around 20 nm. The size distribution of the B-HT and C-HT UCNPs is broader than that of the D-HT and TD UCNPs, while the largest size distribution was observed in the case of the A-HT UCNPs. We can conclude that the ligands, like OA (TD) or PEG (D-HT), which limit the particle growth, also affect the size distribution, probably by minimizing the secondary growth. As suggested by the SAED, the UCNPs are well crystallized with a cubic (B-HT, C-HT and D-HT) or hexagonal structure (TD) for the $NaYF_4$, which is in accordance with the XRD analyses. Note that the A-HT UCNPs were too thick for the SAED analysis.

The EDXS analyses of the samples confirmed the presence of all the constituent elements, including a minor fraction of O. The later may originate from the surface ligands (CA, PEG or OA). The incorporation of dopants (Yb^{3+},Tm^{3+}) into the $NaYF_4$ matrix was also suggested by the UC emission spectra (Figure 5).

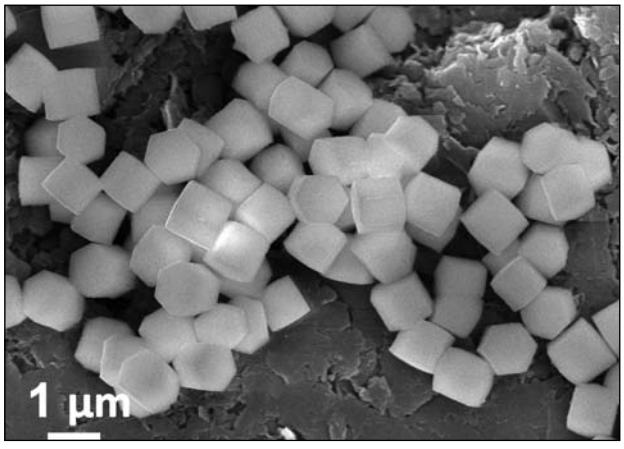

Fig. 4: SEM image of A-HT UCNPs.

The characteristic emission peaks of the Tm^{3+} ions are clearly observed in Figure 5. The dominant emission peak in the NIR at 800 nm, can be attributed to the electronic transition from $^3H_4$ to $^3H_6$, and the weaker blue emission at 475 nm, can be attributed to the electronic transition from $^1G_4$ to $^3H_6$. Six individual transitions were identified within the emission band at 800 nm, with peaks at 770, 782, 793, 800, 817, and ~834 nm. This is in agreement with the potential for 6-fold splitting of the Tm^{3+} ground-state manifold $^3H_6$. The spectral structure of the emission at 800 nm provides a valuable insight into the interaction of the Tm^{3+} electronic levels involved in the respective radiative transition with the local crystal field. For example, the broadening of the individual emission peaks of the HT samples in comparison to the TD sample indicates a lower degree in the crystal order of the HT UCNPs. The strongest NIR emission at 800 nm was observed for the TD UCNPs. Here, only three of the above mentioned transitions are observed, with the 800 nm peak dominating over the peaks at 872 nm and 817 nm. However, in the case of the C-HT it is clear that the intensities of the peaks at 872 and 817 nm are greater than the peak at 800 nm. Similar to this, the B-HT and D-HT UCNPs show a dominant emission at 817 nm. The small peak at 642 nm can be assigned to the electronic transition of $^1G_4$ to $^3F_4$, and the small peaks at 582 nm, 657 and 592 nm can be attributed to impurities originating from the reagents. To conclude, the NIR emission at around 800 nm for the UCNPs is much stronger than for the visible light, which

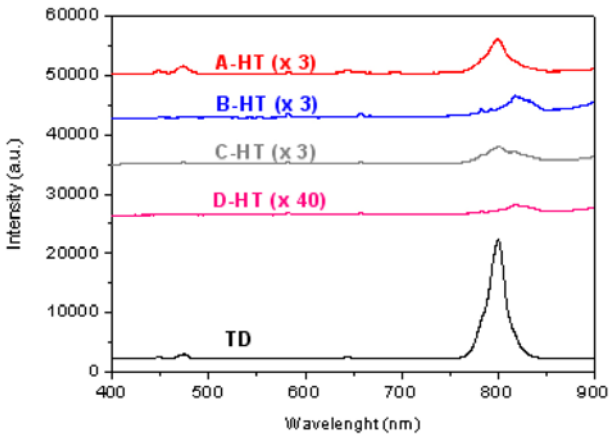

Fig. 5: UC fluorescence spectra of UCNPs in aqueous suspensions. In order to make the weak fluorescence of the samples HT more easily seen, their spectra were multiplied by a factor of 3 (A-HT, B-HT and C-HT) or by a factor of 40 (D-HT).

makes the studied UCNPs suitable candidates for bio-applications.[17,31]

Dissolved fluoride (F^-), Y^{3+}, RE (Yb^{3+} and Tm^{3+}) and sodium (Na^+) ions were detected in the aqueous suspensions of all the synthesized UCNPs, regardless of their size, crystal structure and the method of synthesis. For a comparison of the different synthesis yields we calculated the molar fraction of dissolved F^- per formula unit (the last column in Table 2). A significantly lower dissolution degree was measured for the TD UCNPs than for the HT UCNPs, which crystallized in a different crystal structure. The highest concentration of F in the D-HT sample solution can be (at least partly) attributed to the remaining water-soluble NaF, which most likely resulted from an inadequate purification step. This also coincides with the highest concentration of dissolved Na^+ and was confirmed by the XRD peak at 2Theta = 38.8° (Figure 2). Nevertheless, the overall dissolution (including RE ions) was the most extensive in the D-HT sample, with the smallest particle size among the α-$NaYF_4$ samples. Otherwise, no significant difference in the dissolution of the $F^-$was detected between the A-HT, B-HT and C-HT UCNPs, regardless of their size. Although the TD UCNPs were the smallest, they showed a superior chemical stability, i.e., the smallest degree of dissolved F^- and other constituent ions.

4. Conclusion

$NaYF_4$ UCNPs co-doped with $Yb^{3+}$and Tm^{3+} with cubic and hexagonal crystal structures were synthesized using the hydrothermal and thermal decomposition methods, respectively. We detected the dissolution of all the UCNPs in water. However, the hydrothermally synthesized UCNPs showed a poorer chemical stability in comparison with those that were synthesized by thermal decomposition. This was attributed to the different crystal structures. The UCNPs that were synthesized by thermal decomposition crystallized in a hexagonal crystal structure, which is thermodynamically stable, as opposed to the hydrothermally synthesized UCNPs, which crystallized in a metastable, cubic crystal structure. At the same time the hexagonal UCNPs showed a more efficient UC emission than the cubic ones. We conclude that among the studied fluoride UCNPs the most suitable for bio-applications are the UCNPs with a hexagonal structure that can be synthesized by thermal decomposition.

5. Acknowledgement

The financial support by the Slovenian Research Agency (research programs P2-0089, P1-0045 and P1-0192) is gratefully acknowledged. The authors also acknowledge the use of equipment in the Centre of Excellence on Nanoscience and Nanotechnology – Nanocenter.

6. References

1. J. H. Rao, A. Dragulescu-Andrasi, H. Q. Yao, *Curr. Opin. Biotechnol.* **2007**, *18*, 17–25. http://dx.doi.org/10.1016/j.copbio.2007.01.003
2. J. Shen, L.D. Sun, C. H. Yan, *Dalton Trans.* **2008**, *42*, 5687–5697. http://dx.doi.org/10.1039/b805306e
3. X. Wang, Y. D. Li, *Chem. Commun.* **2007**, *28*, 2901–2910. http://dx.doi.org/10.1039/b700183e
4. F. Auzel, **2004**, *Chem. Rev. 104*, 139–173. http://dx.doi.org/10.1021/cr020357g
5. F. Wang, X. G. Liu, *Chem. Soc. Rev.* **2009**, *38*, 976–989. http://dx.doi.org/10.1039/b809132n
6. F. Vetrone, J. A. Capobianco, *Int J Nanotechnol* **2008**, 5, 1309–1339. http://dx.doi.org/10.1504/IJNT.2008.019840
7. F. Wang, D. Banerjee, Y. S. Liu, X. Y. Chen, X. G. Liu, *Analyst* **2010**, *135*, 1839–1854. http://dx.doi.org/10.1039/c0an00144a
8. C. X. Li, J. Lin, *J. Mater. Chem.* **2010**, *20*, 6831–6847. http://dx.doi.org/10.1039/c0jm00031k
9. J. C. G. Bunzli, *Chem. Rev.* **2010**, *110*, 2729–2755. http://dx.doi.org/10.1021/cr900362e
10. F. Wang, D. Banerjee, Y. Liu, X. Chen, X. Liu, *Analyst* **2010**, *135*, 1839–1854. http://dx.doi.org/10.1039/c0an00144a
11. C. Bouzigues, T. Gacoin, A. Alexandrou, *ACS Nano* **2011**, *5*, 8488–8505. http://dx.doi.org/10.1021/nn202378b
12. M. Wang, G. Abbineni, A. Clevenger, C. Mao, S. Xu, *Nanomedicine: NBM* **2011**, *7*, 710–729. http://dx.doi.org/10.1016/j.nano.2011.02.013
13. J. Zhou, Z. Liu, F. Li, *Chem Soc Rev* **2012**, *41*, 1323–1349. http://dx.doi.org/10.1039/C1CS15187H
14. C. Li, Z. Quan, J. Yang, P. Yang, J. Lin, *Inorg. Chem.* **2007**, *46(16)*, 6329–6337. http://dx.doi.org/10.1021/ic070335i

15. H. S. Qian, Y. Zhang *Langmuir* **2008**, *24*, 12123–12125.
16. C Wang, X. Cheng, *J. Alloys Compd.* **2014**, *617*, 807–815. http://dx.doi.org/10.1016/j.jallcom.2014.08.101
17. J. C. Boyer, L. A. Cuccia, J. A. Capobianco, *Nano Lett.* **2007**, *7(3),* 847–852. http://dx.doi.org/10.1021/nl070235+
18. M. Nyk, R. Kumar, T. Y. Ohulchanskyy, E. J. Bergey, P. N. Prasad, *Nano Lett.* **2008**, *8*, 3834. http://dx.doi.org/10.1021/nl802223f
19. J. Li, X. Chang, X. Chen, Z. Gu, F. Zhao, Z. Chai, Y. Zhao, *Biotechnol. Adv.* **2014**, *32*,727–743. http://dx.doi.org/10.1016/j.biotechadv.2013.12.009
20. T. Mirkovic, M. A. Hines, P.S. Nair, G. D. Scholes, *Chem. Mater* **2005**, *17*, 3451–3456. http://dx.doi.org/10.1021/cm048064m
21. J. Shan, W. Kong, R. Wei, N. Yao, Y. Ju, *J. Appl. Phys.* **2010**, *107*, 054901. http://dx.doi.org/10.1063/1.3298905
22. Y. F. Wang, L.D. Sun, J. W. Xiao, W. Feng, J. C. Zhou, J. Shen, C. H. Yan, *Chem. Eur. J.* **2012**, *18*, 5558–5564. http://dx.doi.org/10.1002/chem.201103485
23. M. Ponikvar-Svet, K. F. Edwards, J. F. Liebman, *Acta Chim. Slov*. **2013**, *60*, 471–483.
24. T. Grobner, *Nephrol. Dial. Transplant*. **2006**, *21*, 1104–1108. http://dx.doi.org/10.1093/ndt/gfk062
25. O. Barbier, L. Arreola-Mendoza, L. M. del Razo, *Chem.-Biol. Interact.* **2010**, *188*, 319–333. http://dx.doi.org/10.1016/j.cbi.2010.07.011
26. H. S. Qian, Y. Zhang, *Langmuir* **2008**, *24*, 12123–12125. http://dx.doi.org/10.1021/la802343f
27. N. Bogdan, F. Vetrone, G.A. Ozin, J. A. Capobianco, *Nano Lett.* **2011**, *11*, 835–840. http://dx.doi.org/10.1021/nl1041929
28. G. S. Pawley, *J. Appl. Crystallogr.* **1981**, *14*, 357–361. http://dx.doi.org/10.1107/S0021889881009618
29. M. Ponikvar, V. Stibilj, B. Žemva, *Food Chem.***2007**, *103*, 369–374. http://dx.doi.org/10.1016/j.foodchem.2006.07.032
30. C. Wang, X. Cheng, *J. Alloys Compd.* **2014**.
31. C. Liu, D. Chen, *J. Mater. Chem.* **2007**, *17*, 3875–3880. http://dx.doi.org/10.1039/b707927c

Povzetek

Fluorescenčni nanodelci, še posebej fluoridni nanodelci, so bili med drugimi optičnimi materiali deležni še posebne pozornosti; v primeru, da je stabilnost delcev v vodi izjemno dobra, je mogoča njihova uporaba v bio-slikanju. Raziskovali smo vpliv sinteznih parametrov na kemijsko stabilnost z Yb^{3+} in Tm^{3+} kodopiranih $NaYF_4$ nanodelcev, ki so bili sintetizirani hidrotermalno ali s termičnim razklopom in so imeli različno kristalno strukturo. Sintetizirane nanodelce smo okarakterizirali z rentgensko praškovno difrakcijo in transmisijsko elektronsko mikroskopijo. Fluorescenco z energijsko pretvorbo navzgor (angl. upconversion) nanodelcev dispregiranih v vodi smo izmerili med 400–900 nm. Delno odtapljanje fluorida smo v vseh vzorcih določali z ionskoselektivno elektrodo in odtapljanje ostalih ionov z optično emisijsko spektroskopijo z induktivno sklopljeno plazmo. Nanodelci sintetizirani s termičnim razklopom s heksagonalno kristalno strukturo in velikostjo približno 20 nm so imeli ne le odlično kemijsko stabilnost v vodi temveč tudi izjemno učinkovitost fluorescence z energijsko pretvorbo navzgor.